Energy Partitioning Studies of CO and NO Chemisorption on the Pd(111) Surface

Wingfield V. Glassey

Department of Chemistry, The College of Wooster, Wooster, Ohio 44691

Received: October 31, 2003; In Final Form: February 6, 2004

A bond-by-bond partitioning of the electron energy within the p(2 × 2)-CO/Pd(111) and p(2 × 2)-NO/Pd-(111) chemisorption systems has been used to demonstrate a preference for CO and NO chemisorption in hollow sites. The changes in bonding within the adsorbate and within the surface that accompany formation of the chemisorption bond are quantified using Hamilton population analysis: a partitioning of the electron energy among the atoms and bonds. In this way, the preference for CO and NO chemisorption in hollow sites is seen to result from the inability of the increased reduction in bonding within both the adsorbate and surface to counter the increase in surface−adsorbate bonding with increasing adsorbate coordination. By comparison with CO chemisorption, the chemisorption of NO is characterized by stronger surface−adsorbate bonding on all sites; principally the result of increased mixing between the NO(2π) orbitals and the surface d band. Increased mixing between the NO(2π) orbitals and the surface d band, in turn, results in increased back-donation to the NO(2π) orbitals on all sites and, correspondingly, a greater degree of bond weakening within NO on all sites. The increase in 2π-d mixing on chemisorbing NO does not, however, result in increased Pd−Pd bond weakening. Instead, increased 2π-d mixing on chemisorbing NO serves to depopulate a greater number of those surface states contributing to d−d antibonding interactions within Pd−Pd bonds about chemisorbed NO. In this way, the analysis of CO and NO chemisorption presented provides new insight into the mechanism by which chemisorbed CO and NO perturb the electronic structure of the surface and, potentially, influence the chemisorption of neighboring adsorbates at higher coverages. Detailed analysis of the adsorbate orbital contributions to Pd−CO and Pd−NO bonding also reveals that both the adsorbate σ and π orbitals mix primarily with the surface s and p bands. Within the context of the molecular orbital picture of CO and NO chemisorption presented, interaction of the adsorbate orbitals with the d band acts only to perturb the more substantial interaction between the adsorbate orbitals and the surface s and p bands. In this way, the molecular orbital picture of CO and NO chemisorption presented serves to validate the d-band model of chemisorption devised previously by Hammer et al.

I. Introduction

In recent years, an increasing number of experimental and computational studies have indicated that both CO and NO favor 3-fold hollow sites when chemisorbed at low to moderate coverages on the Pd(111) surface. Many such studies have prompted a reevaluation of existing data indicating a preference for chemisorption on top and/or bridging sites. Recent photoelectron diffraction studies of the CO/Pd(111) chemisorption by Giessel et al.[1] point to the existence of well defined ($\sqrt{3} \times \sqrt{3}$) *R*30° and c(4 × 2) overlayer structures at, respectively, one-third and one-half coverage. Formation of the ($\sqrt{3} \times \sqrt{3}$) *R*30° phase at one-third coverage is attributed to the chemisorption of CO in fcc hollow sites in accord with prior LEED studies by Ohtani et al.[2] In their photoelectron diffraction study, Giessel et al.[1] attribute the formation of the ordered c(4 × 2) overlayer structure at one-half monolayer coverage to the occupation of both hcp and fcc hollow sites in approximately equal numbers. The mixed fcc-hcp model of the c(4 × 2)-2CO/Pd(111) chemisorption system proposed by Giessel et al. is further supported by the computational studies of Loffreda et al.[3] Mixed hcp-fcc site occupation for CO at half-coverage is further supported by the modest 0.03 eV preference for CO chemisorption in fcc sites over hcp sites at one-third coverage computed by Sautet et al.[4] The assignment of CO to fcc and/or hcp hollow sites contrasts prior interpretations of IR and LEED data on which it was proposed that CO occupies solely bridging sites in the c(4 × 2) phase at half-coverage.[5−8]

Recent studies of NO chemisorption on the Pd(111) surface also demonstrate a preference for chemisorption in fcc sites within the ($\sqrt{3} \times \sqrt{3}$) *R*30° phase observed at one-third coverage and mixed fcc-hcp site occupation in the c(4 × 2) phase formed at half-coverage.[9,10] As was the case for CO chemisorption on the Pd(111) surface, the assignment of NO to fcc and/or hcp sites contrasts earlier assignments in favor of NO chemisorption in bridging[11−13] and top[14] sites.

The initial focus of the present work is to rationalize the preference for CO and NO chemisorption in hollow sites. The electronic structure changes accompanying CO and NO chemisorption are analyzed using Hamilton population (HP) analysis, a partitioning of the electronic energy among the atoms and bonds, within a one-electron tightbinding framework.[15,16] In this way, it becomes possible to quantify the extent to which the changes in Pd−Pd bonding within the surface and the changes in bonding within the adsorbate that accompany chemisorption modify the strength of the surface−adsorbate chemisorption bond and, by so doing, determine the chemisorption site preference for CO and NO on the Pd(111) surface. Application of the HP methodology serves to unambiguously quantify and localize the changes in bonding accompanying chemisorption, and as such, affords a more chemically intuitive interpretation

10.1021/jp031217t CCC: $27.50
Published on Web 04/20/2004

TABLE 1: Pd−C and Pd−N Bond Lengths Used to Model the p(2 × 2)-CO/Pd(111) and NO/Pd(111) Chemisorption Systems[a]

site	Pd−C/Å	Pd−N/Å
top	1.89	1.93
bridge	2.03	2.03
hcp	2.10	2.08
fcc	2.10	2.08

[a] All bond lengths are taken from the DFT study by Honkala et al.[17]

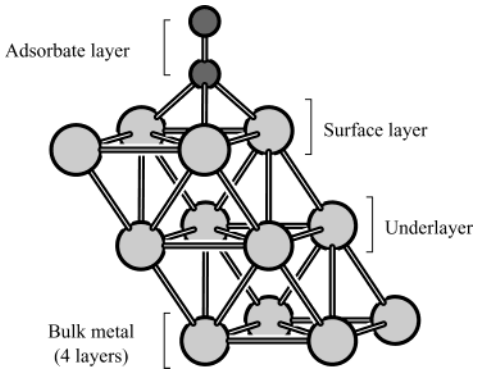

Figure 1. Geometric partitioning of the p(2 × 2) supercell into adsorbate, surface layer, underlayer, and bulk metal fragments. Layers 4, 5, and 6 of the Pd slab (not shown) are part of the bulk metal fragment.

of chemisorption site preference than that afforded by more rigorous but generally less amenable methodologies such as density functional theory.

The present study also serves to highlight the mechanism by which the interactions between individual CO and NO orbitals and the surface bands modify the electronic structure within individual Pd−Pd bonds about chemisorbed CO or NO. Within the HP formalism, individual bond energies can be partitioned into contributions resulting from the interactions between the valence orbitals of the atoms defining the bond. Thus, comparison of the s-, p-, and d-orbital contributions to Pd−Pd bonding in the Pd−Pd bonds about chemisorbed CO or NO with their respective contributions in the absence of the adsorbate provides detailed insight into the mechanism by which chemisorption perturbs the electronic structure of the surface. Such information regarding the nature and spatial extent of perturbations in the surface electronic structure accompanying chemisorption is expected to provide new and valuable insight into the mechanism by which the interactions between coadsorbed molecules are mediated by the intervening surface.

II. Computational Methods

The chemisorption of CO and NO on the Pd(111) surface was modeled using 6-layer slab models based on a p(2 × 2) supercell. The slab models were constructed using the bulk Pd bond length of 3.89 Å. The top, bridge, and hollow site geometries for CO and NO were constructed using the Pd−C and Pd−N bond lengths calculated by Honkala et al. using DFT.[17] The bond lengths are summarized in Table 1.

The supercell contents were partitioned into several geometric fragments according to the scheme given in Figure 1. The geometric partitioning shown in Figure 1 serves to focus attention on the extent to which the changes in bonding within the slab are localized within the vicinity of the adsorbate on binding CO and NO.

Analysis of the electronic structure changes accompanying chemisorption was carried out using a tightbinding implementation of the extended Hückel method.[15] The irreducible wedge of the Brillouin zone was sampled using a 4 × 4 × 1 Monkhorst-Pack *k*-point mesh.[18] The extended Hückel parameters used in the study are summarized in the Appendix. Within the one-electron tightbinding scheme employed, the total electronic energy can be readily partitioned into one and two-center "atom" and "bond" contributions according to the equation

$$E_{\mathrm{tot}} = \sum_{\substack{\mathrm{atoms}\\ i}} \mathrm{AHP}_i + \sum_{\substack{\mathrm{atoms}\\ i}} \sum_{\substack{\mathrm{atoms}\\ j}} \mathrm{BHP}_{ij} \qquad (1)$$

In eq 1, the abbreviations AHP and BHP are used to denote individual atom and bond contributions to the total energy: the so-called atom and bond Hamilton populations. The atom and bond HPs, as defined by eq 1, are extracted from the band-structure of the combined slab and adsorbate layer. The atom HP for an atom (*i*), AHP_i, refers to the component of the electron energy that results from electron occupation of the valence orbitals of the atom. The bond HP between two atoms (*i* and *j*), BHP_{ij}, refers to the contribution to the electron energy resulting from the interaction between the atomic basis functions of one atom (*i*) with those on the other (*j*). In the HP formalism, bonding (stabilizing) interactions between orbitals on two different atoms result in negative contributions to the bond energy (BHP) between the atoms. Conversely, antibonding (destabilizing) orbital interactions between atoms result in positive contributions to the BHP between the atoms.

On adopting the supercell partitioning shown in Figure 1, the atom-bond energy partitioning of eq 1 affords the opportunity to define the energy of each geometric fragment and, in so doing, construct the total electronic energy to be the sum of individual fragment energies, so-called fragment Hamilton populations (FHPs), and the interactions between fragments according to the equation

$$E_{\mathrm{tot}} = \sum_{\substack{\mathrm{fragments}\\ i}} \mathrm{FHP}_{\mathrm{i}} + \sum_{\substack{\mathrm{fragments}\\ i}} \sum_{\substack{\mathrm{fragments}\\ j}} \mathrm{FHP}_{i-j} \qquad (2)$$

According to the atom-bond partitioning of eq 1, every atom in the structure has an energy defined by its AHP. Further, every atom (*i*) in the structure interacts with every other atom ($j \neq i$), as defined by the corresponding bond HPs, BHP_{ij}. Thus, if the atom-bond partitioning scheme of eq 1 is to be recast in the form of eq 2, the energy of a user-defined group of atoms or "fragment" (FHP_i) refers to the sum of the atom energies (AHPs) for the constituent atoms and those BHPs between atoms belonging to the fragment. Thus, in the case of CO chemisorption, the fragment energy for CO is comprised not only of the C and O atom energies (AHPs) but the energy of the C−O bond between the two atoms defining the fragment. It is also important to note a third contribution to the fragment energy that has particular significance in the present case. The CO fragment HP also includes the sum of the BHPs between the C and O atoms in the supercell, which we refer to as the CO fragment, and their mirrors within those CO molecules in surrounding supercells. Thus, on extracting this component of the CO fragment HP, it becomes possible to quantify the extent of through-space interactions between CO molecules chemisorbed on the surface.

On extracting those BHPs contributing to the energies of individual fragments from eq 1, only those BHPs defining the interactions between atoms in different fragments remain. Grouping these BHPs yields the interfragment HPs, $\mathrm{FHP}_{ij}(i \neq j)$ −

each defining the net bond HP between the sets of atoms defining two different fragments (*i* and *j*). As was the case with individual BHPs, a negative HP between fragments refers to a net bonding interaction between fragments.

Applying the fragment energy partitioning of eq 2 to the geometric partitioning in Figure 1 yields

$$E_{tot} = FHP_{ads} + FHP_s + FHP_u + FHP_b + FHP_{ads-s} + FHP_{ads-u} + FHP_{ads-b} + FHP_{s-u} + FHP_{s-b} + FHP_{u-b} \quad (3)$$

In eq 3, the labels ads, s, u, and b are used to refer to the adsorbate, the surface layer, the underlayer, and the bulk layers as defined by the partitioning in Figure 1. Thus, there are potentially 10 contributions to the total electronic energy that result from the geometric partitioning of the p(2 × 2) supercell in Figure 1. Analysis of the changes in each of the fragment populations given in eq 3 on chemisorbing CO and NO reveals that in excess of 99% of the Pd−Pd bonding changes resulting from chemisorption are localized in the Pd−Pd bonds within the surface layer and those Pd−Pd bonds between the surface layer and the underlayer. Equation 3 can be further simplified on noting that the interactions between adsorbates and the atoms in the underlayer account for less than 1% of the total adsorbate−slab interaction. On choosing to make this approximation, the surface−adsorbate HPs (FHP_{ads-s}) reported in this study are accurate only to within ± 0.05 eV. Individual AHPs, BHPs, and FHPs are computed to at least six decimal places; however, in the implementation of the HP method used in this study, they are reported to only two decimal places in the output and as such, when using individual atom, bond, or fragment HPs, each has an associated uncertainty of ±0.01 eV. In this way, the interaction between the surface layer and the bulk layers of the slab (less than 0.01 eV) is not significant and can be neglected.

Thus, it becomes possible to account for in excess of 99% of the total bond HP changes occurring on chemisorption by considering only the change in the adsorbate and surface FHPs (FHP_a and FHP_s), the change in the FHP describing the surface−adsorbate bond (FHP_{ads-s}), and the change in the FHP describing bonding between the surface and underlayer (FHP_{s-u}).

Having clearly defined the nature of the partitioning scheme and the partitioning of the supercell contents, the focus shifts to the construction of a chemically intuitive measure of chemisorption energy.

III. CO Chemisorption

Given the preference for CO chemisorption in hollow sites within both the ($\sqrt{3} \times \sqrt{3}$) *R*30° phase at one-third monolayer coverage and the ordered c(4 × 2) phase at half-monolayer coverage,[1,3] it becomes necessary to establish the energetic preference for hollow site chemisorption within the framework of the energy partitioning scheme introduced in the previous section.

From a computational perspective, the chemisorption energy, E_{chem}, is modeled by the difference in the total energy of the chemisorption system (slab plus adsorbate layer) relative to that of the slab and adsorbate layer taken separately i.e.

$$E_{chem} = E_{tot}(CO/Pd) - E_{tot}(Pd) - E_{tot}(CO) \quad (4)$$

Prior HP studies of CO chemisorption on the Pt, Cu, and Al(111) surfaces[19] demonstrate that, at one-quarter coverage, the portion of the CO fragment population (FHP_{co}) describing direct (through-space) interactions between neighboring CO molecules is less than 0.01 eV − the programmed uncertainty in the HP method − and, as such, is considered negligible. Thus, to model the energetics of CO chemisorption on these surfaces, it is only necessary to consider the strength of the Pd−CO interaction, the change in C−O bonding within the CO fragment, and the change in Pd−Pd bonding within the slab on chemisorbing CO. The same is found to be true for NO chemisorption on the Pd(111) surface at one-quarter coverage, and it becomes instructive to write an additional expression for the chemisorption energy of the form

$$E_{chem} = HP(Pd-CO) + \Delta HP(C-O) + \Delta HP(Pd-Pd) \quad (5)$$

In eq 5 the Pd−CO interaction is denoted HP(Pd−CO) and, as discussed previously, is defined by the FHP between the surface layer and chemisorbed CO, FHP_{co-s}. In the absence of a significant interaction between neighboring CO molecules, ΔHP(C−O) refers only to the variation in the C−O BHP within the CO fragment on introducing the metal slab. Finally, the changes in Pd−Pd bonding accompanying CO and NO chemisorption are confined to the Pd−Pd bonds within the surface layer and the Pd−Pd bonds between those atoms in the surface layer and those of the underlayer. The change in bonding within the slab on chemisorbing CO, ΔHP(Pd−Pd) thus refers to the combined change in the BHP component of the FHP for the surface layer (FHP_s) and the FHP between the surface layer and underlayer (FHP_{s-u}).

The chemisorption energies for top, bridge, and hollow site CO chemisorption computed using eq 5 are summarized in Table 2. The contributions to ΔHP(Pd−Pd) derived from changes in Pd−Pd bonding within the surface layer (ΔHP_s) and between the surface layer and the underlayer (ΔHP_{s-u}), are listed separately. The HP analysis summarized in Table 2 demonstrates a significant energetic preference for CO chemisorption in hollow sites over bridge sites, in agreement with the findings of prior studies.[1,3,4,17] Given that each contribution to the chemisorption energy reported in Table 2 has an associated 0.01 eV uncertainty, the marginal preference computed for chemisorption in hcp sites over fcc sites is statistically insignificant. This is especially true on considering the additional 0.05 eV uncertainty that results from the neglect of interactions between the adsorbate and the underlayer. In this way, this result reflects both the modest 0.03 eV preference for CO chemisorption in fcc sites over hcp sites computed by Sautet et al.[4] and the absence of a preference for one site over the other as computed by Honkala et al.[17] Further, the lack of a significant preference for chemisorption in one type of hollow site over the other also helps to rationalize the recent photoelectron diffraction studies by Giessel et al.[1] revealing mixed hcp-fcc site adsorption for CO chemisorbed at half coverage on Pd(111).

TABLE 2: Decomposition of the Computed CO Chemisorption Energies for p(2 × 2)-CO/Pd(111) Chemisorption Systems with CO Chemisorbed in Top, Bridge, and Hollow Sites[a]

			ΔHP(Pd−Pd)		
CO site	HP(Pd−CO)	ΔHP(C−O)	ΔHP_s	ΔHP_{s-u}	E_{chem}
top	−16.85	0.75	0.41	0.62	−15.07
bridge	−20.51	2.27	1.86	0.92	−15.46
hcp	−21.95	2.86	2.21	1.16	−15.72
fcc	−21.86	2.80	2.34	1.04	−15.68

[a] All HPs are in units of eV. The change in Pd−Pd bonding within the slab, ΔHP(Pd−Pd) is decomposed to reveal the change in Pd−Pd bonding within the surface (ΔHP_s) and between the surface and underlayer (ΔHP_{s-u}).

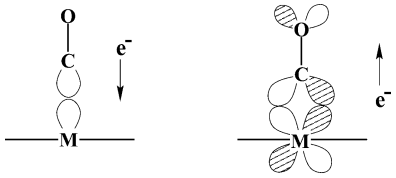

Figure 2. Blyholder model of CO chemisorption on transition metal surfaces.

TABLE 3: Individual CO Orbital Contributions to the Pd−CO Bond HP for the p(2 × 2)-CO/Pd(111) Chemisorption System with CO on Bridging Sites

	Pd-CO HP/eV			
CO orbital	top	bridge	HCP hollow	FCC hollow
3σ	0.257	0.737	0.937	0.938
4σ	−4.287	−4.546	−4.690	−4.671
1π	0.226	0.182	0.120	0.112
5σ	−9.104	−9.290	−9.395	−9.403
2π	−3.857	−7.406	−8.709	−8.633
6σ	−0.082	−0.185	−0.210	−0.208
total	−16.847	−20.508	−21.947	−21.865
$4\sigma + 5\sigma + 2\pi$	−17.248	−21.242	−22.794	−22.707

Given that the HP method is capable of reproducing the energetic preference for hollow site chemisorption and does not discern a significant preference for chemisorption in either fcc or hcp sites, it proves instructive to attempt an analysis of the electronic structure changes that, when taken as a whole, result in a preference for hollow site chemisorption.

Traditionally, the surface-CO chemisorption bond is described using the Blyholder model.[20] In the Blyholder model, CO binding to the metal surface is the result of a synergistic donation of electrons from the HOMO, the 5σ orbital, to the surface accompanied by the back-donation of electrons from the surface d band to the CO(2π) orbital, the LUMO, as illustrated in Figure 2. Prior application of HP analysis to CO chemisorption on the Ni(100)[15] and M(111); M = Pt, Cu, and Al surfaces[19] indicates that, from both a qualitative and quantitative standpoint, it is necessary to extend the Blyholder model by explicitly considering surface−CO interactions involving both the CO(4σ) orbital and the surface s and p bands.

Within the one-electron tightbinding scheme employed in this study,[15] it is possible to decompose the Pd−CO bond HP into the contributions from individual CO molecular orbitals. The resulting contributions to Pd−CO bonding are summarized in Table 3 for p(2 × 2) coverages of CO chemisorbed in top, bridge, and hollow sites. Analysis of Table 3 reveals that, on each chemisorption site, the interactions between the CO 4σ, 5σ, and 2π orbitals and the surface are significant. The results in Table 3 further indicate that, on each site, the 4σ orbital contributes approximately one-third of the total σ interaction and, as such, is a significant contributor to σ bonding between the surface and CO. Prior HP studies of CO chemisorption on the Pt, Cu, and Al(111) surfaces[19] also reveal that the CO(4σ) orbital is responsible for approximately one-third of the total σ interaction between CO and the surface. The substantial increase in the HPs describing the interaction between individual CO orbitals and the surface bands with increasing CO coordination (Table 3) is attributed to increased overlap between the CO orbitals and the surface bands.[21,22] The effects of increased overlap with increasing coordination are particularly evident for the Pd−CO(2π) interaction. Analysis of the CO orbital contributions to Pd−CO bonding shown in Table 3 reveals that the

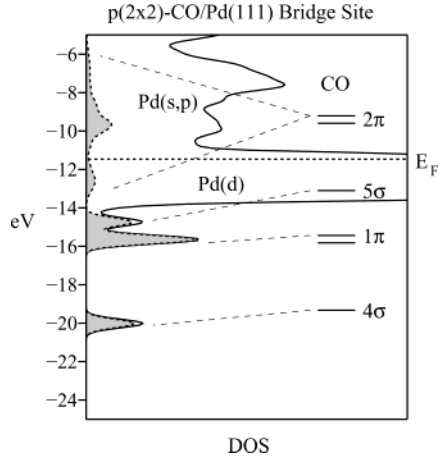

Figure 3. DOS for the p(2 × 2)-CO/Pd(111) chemisorption system with CO chemisorbed in bridging sites. Contributions from the CO orbitals are shown shaded. The molecular orbital energies for an isolated gas-phase CO molecule are superimposed for comparison.

TABLE 4: CO 4σ, 5σ, and 2π Orbital Occupations for p(2 × 2)-CO/Pd(111) Phases with CO Chemisorbed in Top, Bridge, and Hollow Sites

	MO occupation			
CO orbital	top	bridge	HCP hollow	FCC hollow
4σ	1.83	1.81	1.80	1.80
5σ	1.62	1.60	1.60	1.60
2π	0.33	0.61	0.71	0.70

CO(2π) orbitals are primarily responsible for the increase in Pd−CO bonding with increasing CO coordination, in accord with prior HP studies of CO chemisorption on the Pt, Cu, and Al(111) surfaces.[19] Given the increased overlap between the CO(2π) orbitals and the surface bands on moving CO to higher coordinate sites, one might expect to observe increased back-donation. The CO(2π) orbital occupations for top, bridge, and hollow site chemisorption summarized in Table 4 demonstrate that this is indeed the case. Increased back-donation, in turn, gives rise to an increased reduction in C−O bonding as evidenced by increased antibonding (positive) contributions to the C−O Hamilton population with increasing coordination (Table 2).

In addition to a reduction in C−O bonding on the higher coordination sites, increased Pd−CO interaction gives rise to an increased reduction in Pd−Pd bonding, both within the surface and between the surface layer and the underlayer (Table 2). Yet, despite increased C−O and Pd−Pd bond weakening, increased Pd−CO bonding with increasing CO coordination results in an energetic preference for CO chemisorption in hollow sites. This contrasts the previously studied case of CO chemisorption on the Pt(111) and Cu(111) surfaces[19] for which the increase in surface−CO bonding with increasing coordination was insufficient to offset the increased reduction in C−O and metal−metal bonding that ultimately resulted in a preference for chemisorption in top sites on both surfaces. A detailed account of the Pd−Pd bonding changes accompanying CO and NO chemisorption is presented following a discussion of NO chemisorption.

The interactions between the CO orbitals and the surface bands are best illustrated in the form of the density of states (DOS) for the CO/Pd(111) chemisorption system. The DOS for the p(2 × 2)-CO/Pd(111) chemisorption system with CO in bridging sites is illustrated in Figure 3. The contributions of the CO 4σ, 5σ, and 2π orbitals to the DOS are shown shaded. Interactions between the energetically low-lying CO 4σ and 5σ

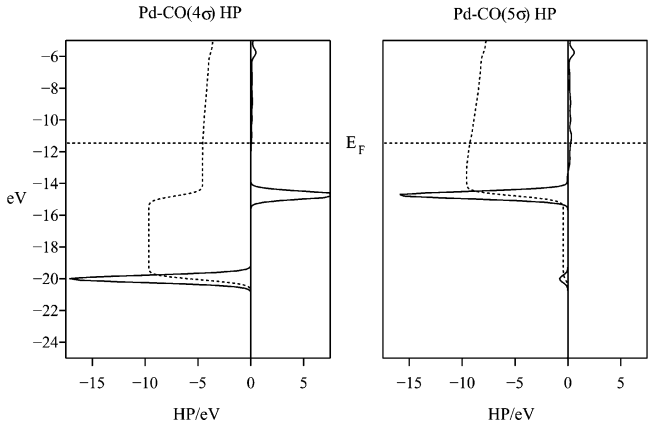

Figure 4. Plots of the energy resolved contributions to the Pd−CO(4σ) and Pd−CO(5σ) HPs. Negative contributions to the HP result from bonding interactions. The net CO(4σ) and CO(5σ) orbital contributions to the Pd−CO bond HP are obtained by summing the contributions to the HP (vertical dashed line) through the Fermi level (horizontal dashed line).

TABLE 5: Surface s-, p-, and d-Band Components of the CO 4σ, 5σ, and 2π Orbital Contributions to the Pd−CO Bond HP for the p(2 × 2)-CO/Pd(111) Chemisorption System with CO on Bridging Sites

	surface band		
CO orbital	Pd(s)	Pd(p)	Pd(d)
4σ	−2.592	−1.519	−0.435
5σ	−4.638	−3.043	−1.609
2π	−1.424	−0.811	−5.171

orbitals and the surface s, p, and d bands give rise to sharp features in the CO/Pd(111) DOS at ∼ −20 and ∼ −15 eV, respectively (Figure 3). Analysis of the energy resolved contributions to the Pd−CO(4σ) HP (Figure 4) reveals a bonding interaction between the surface bands and the CO(4σ) orbital at ∼ −20 eV. Analysis of the Pd−CO(5σ) HP (Figure 4) reveals substantial bonding interactions between the surface bands and the CO(5σ) orbital at ∼ −15 eV. Prior HP studies of the CO/Ni(100)[15] and CO/M(111); M = Pt,Cu,Al chemisorption systems[19] highlight a significant degree of mixing between the CO 4σ and 5σ orbitals on binding CO to the surface. The presence of 4σ−5σ mixing in the CO/Pd(111) chemisorption system is once more evidenced in Figure 4 by the presence of both a reduction in the Pd−CO(4σ) HP resulting from mixing of the CO(4σ) orbital into the Pd−CO(5σ) bonding band at ∼ −15 eV and an increase in Pd−CO(5σ) bonding resulting from mixing of the CO(5σ) orbital into the Pd−CO(4σ) bonding band at ∼ −20 eV. Prior HP studies of CO chemisorption on Pt, Cu, and Al(111) surfaces[19] also reveal that the bonding potential of the CO(4σ) orbital is reduced by approximately 50% by its mixing into the 5σ band at ∼ −15 eV. Figure 4 demonstrates that the same is true for CO chemisorption on Pd(111). Integration of the CO(4σ) HP curve indicates that the CO(4σ) bonding contribution is reduced by 53% on mixing with the 5σ band.

The surface s, p, and d band contributions to the interaction between the surface and the CO 4σ, 5σ, and 2π orbitals are summarized in Table 5. Analysis of Table 5 reveals that the CO 4σ and 5σ orbitals interact with the surface s, p, and, to a lesser extent, d band in agreement with prior HP studies of CO chemisorption on Ni, Pt, Cu, and Al surfaces.[15,19] In contrast, the π component of Pd−CO bonding is dominated by the interaction between the CO(2π) MOs and the surface d band, again in accord with prior HP studies of CO chemisorption on the Ni(100) and Pt(111) surfaces.[15,19]

In the d-band model proposed by Hammer et al.,[23] both the 5σ and 2π CO orbitals interact principally with the surface s and p bands. Their interaction with the surface is subsequently modified through interactions with the d band. The dominant contributions of the surface s and p bands to the sigma component of the Pd−CO bond HP is clearly in accord with their model. However, it is less obvious as to how the HP description of the interaction between the Pd surface bands and the CO(2π) orbitals might conform.

The Pd−CO(2π) HP plots shown in Figure 5 reveal substantial 2π−d bonding interactions distributed throughout the d band. The corresponding 2π−d antibonding states are found in the ∼3 eV window above the Fermi level and are unoccupied. Analysis of the Pd−CO(2π) HPs in Figure 5 reveals significant mixing of the CO(2π) orbitals with the surface s and p bands throughout the ∼3 eV energy window above the Fermi level. Previously, HP analysis has been used to demonstrate that partial filling of these states in the CO/Cu(111) chemisorption system results in strong interaction between the CO(2π) orbitals and the surface s and p bands.[19] The prominent role of the surface s and p bands in binding CO to copper surfaces has also been described previously by Bagus and Pacchioni.[24] Thus, in the case of CO chemisorption on the Pd(111) surface, and previous

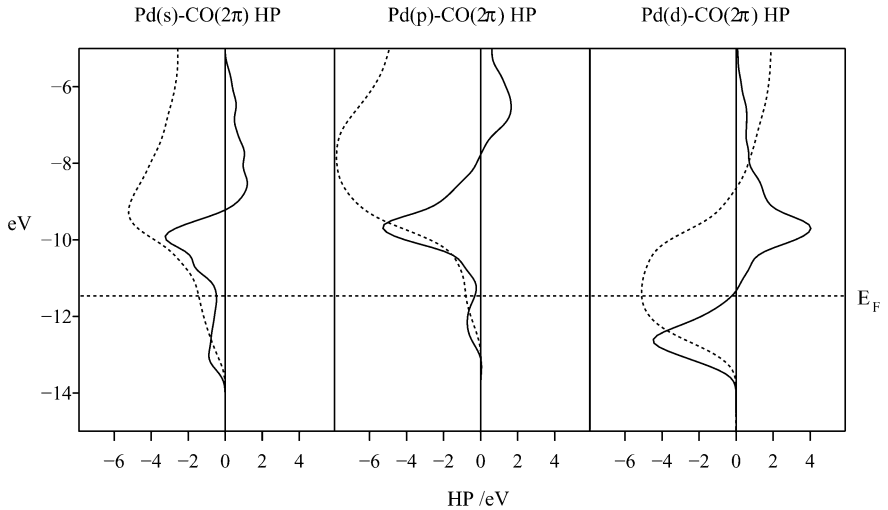

Figure 5. Plots of the energy resolved contributions to the surface s-, p-, and d-band components of the Pd−CO(2π) HP. Bonding contributions to the HP plots appear as negative contributions.

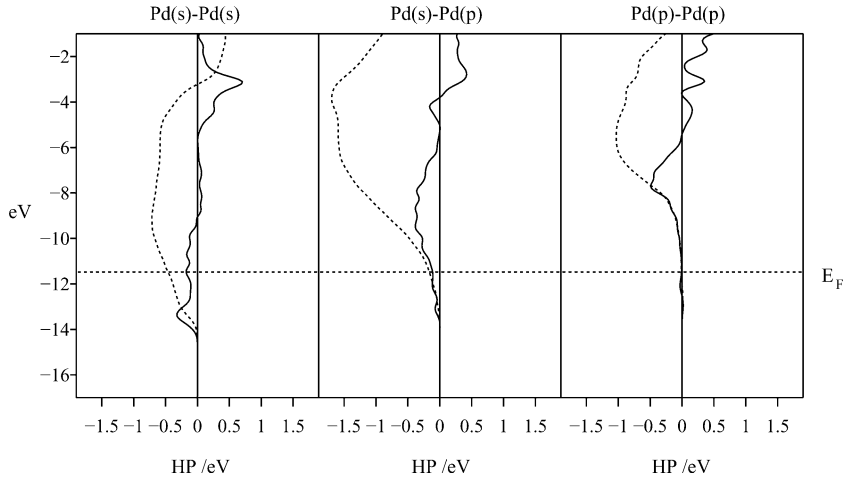

Figure 6. Energy resolved plots of the s−s, s−p, and p−p contributions to the bond HP between neighboring surface atoms in a 6 layer Pd slab. Bonding contributions appear negative.

studies of CO chemisorption on the Ni(100) and Pt(111) surfaces,[15,19] only the 2π−d bonding states distributed throughout the d band are filled. In this way, the CO(2π) orbitals are seen to interact primarily with the surface d band despite substantial mixing of the CO(2π) orbitals with the surface s and p bands in accord with the d-band model proposed by Hammer et al.[23]

IV. Pd−Pd Bonding

Before attempting to describe the changes in Pd−Pd bonding throughout the slab on chemisorbing CO or NO, it is first necessary to develop a model with which to describe metal−metal bonding within a single Pd−Pd bond in the surface. In order to assess the respective contributions of the surface s, p, and d bands to Pd−Pd bonding within the surface, it proves instructive to plot the energy resolved contributions to the interactions between the s, p, and d orbitals on neighboring Pd atoms. The energy resolved contributions to the s−s, s−p, and p−p components of the Pd−Pd bond HP between a pair of neighboring Pd atoms in the surface layer of the slab are shown in Figure 6. Analysis of the s−s component of the Pd−Pd BHP reveals s−s bonding states distributed about the Fermi level between approximately −9 and −14 eV. The corresponding antibonding states are concentrated in the energy window above −5 eV. In contrast to the significant number of s−s bonding states below the Fermi level, the p−p component of the Pd−Pd BHP (Figure 6) reveals that essentially all of the p−p bonding and antibonding states are located above the Fermi level. The p−p bonding interactions are found between −6 and −10 eV. The corresponding antibonding interactions are found above −6 eV. Integration of the p-band DOS (Figure 7) reveals that only 4% of the surface p band is filled. Contributions to the p-band DOS below the Fermi level result from mixing of the p band into the s and d bands. Analysis of the s−p contribution to the surface Pd−Pd bond HP shown in Figure 6 reveals substantial s−p bonding interactions distributed throughout the energy window spanned by the s−s and p−p bonding bands. The electronic structure of the surface s and p bands is summarized in Scheme 1.

Given that the overlap between d orbitals on neighboring Pd atoms within the slab is a full order of magnitude less than either the overlap between the s or p orbitals on neighboring Pd atoms, it is reasonable to expect the d-band width to be significantly less than either the s- or p-band width. Analysis of the d−d component of the Pd−Pd HP between a pair of neighboring

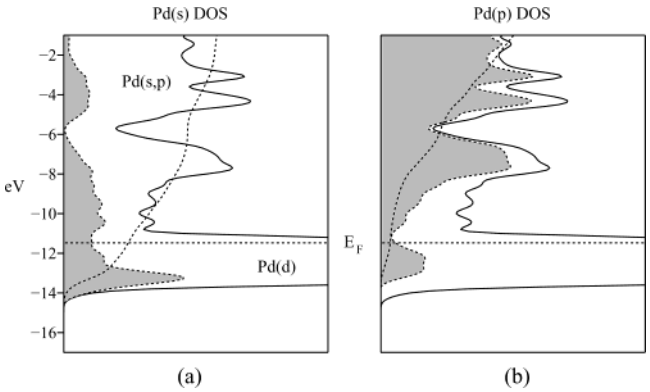

Figure 7. DOS for a 6 layer Pd(111) slab. The surface s- and p-band contributions to the total DOS are shown (shaded) in panels a and b, respectively. Integration of the s- and p-band contributions to the DOS (vertical dashed lines) demonstrates that the majority of the surface s and p bands are located above the Fermi level.

SCHEME 1

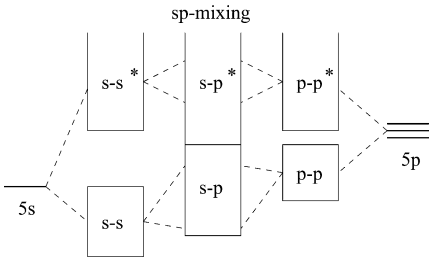

surface atoms (Figure 8) demonstrates the formation of a composite d-band comprised of closely spaced d−d bonding and antibonding bands. The increase in d−d bonding that results from filling the d−d bonding states in the lower portion of the d band is offset by the reduction in d−d bonding on filling many of the d−d antibonding states in the upper portion of the d band. Analysis of the d−d contribution to the Pd−Pd BHP reveals that filling the d−d bonding states and many of the d−d antibonding states results in a net reduction in the Pd−Pd bond HP equivalent to 3% of the total BHP. The surface s-, p-, and d-band contributions to Pd−Pd bonding are summarized in Scheme 2. The bonding and antibonding interactions resulting from sp-mixing shown in Scheme 1 are present but not shown in Scheme 2 in the interest of clarity.

In addition to involvement in s−p mixing, the surface p band mixes with the d band as evidenced by the substantial p−d

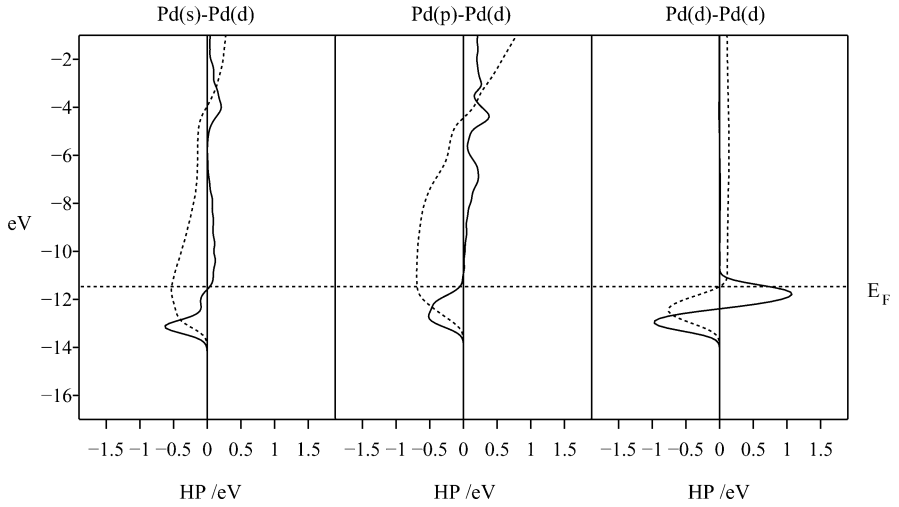

Figure 8. Energy resolved plots of the s−d, p−d, and d−d contributions to the bond HP between neighboring surface atoms in a 6 layer Pd slab. Bonding contributions appear negative.

SCHEME 2

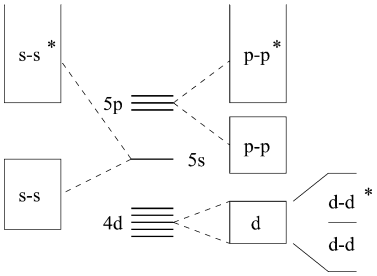

bonding interactions distributed throughout the d band in the p−d component of the Pd−Pd BHP shown in Figure 8. The s−p and p−d contributions to the Pd−Pd bond HP account for 9% and 38% of the total BHP, respectively. In this way, a modest 4% filling of the surface p band can be seen to translate into p-band contributions totaling 47% of the total bond HP.

Integration of the s−s contribution to the total bond HP (Figure 6) reveals that s−s bonding interactions below the Fermi level account for 25% of the total Pd−Pd BHP. By analogy with the p band, the s-band contribution to the total Pd−Pd BHP is significantly enhanced by mixing. In addition to the bonding contributions to the Pd−Pd BHP resulting from sp mixing, mixing of the s band into the lower-lying d band results in substantial s−d bonding interactions. Taken together, the s−p and s−d contributions account for 38% of the total Pd−Pd BHP.

The distribution of the s and p band DOS shown in Figure 7 further reveals that, in contrast to the more uniform mixing of the p band throughout the d band, the s band mixes preferentially with surface d states toward the bottom of the d band. This is reflected in the distribution of the s−d and p−d contributions to the Pd−Pd bond HP shown in Figure 8. Analysis of the s−d component of the Pd−Pd BHP (Figure 8) reveals that the majority of s−d mixing occurs in the lower portion of the d band containing d−d bonding contributions to the Pd−Pd BHP. This contrasts the approximately equally weighted p−d bonding contributions dispersed throughout the d−d bonding and antibonding portions of the d band (Figure 8). Given the description of the surface electronic structure for the Pd(111) slab detailed in Scheme 2, it is practical to attempt a description of the role of the surface s, p, and d bands in Pd−CO bonding and the resulting perturbation of Pd−Pd bonding about chemisorbed CO.

V. Pd−CO Bonding

Given the description of Pd−Pd bonding outlined in the previous section, it becomes possible to account for the extent of mixing between individual adsorbate orbitals and the surface s, p, and d bands. Consider first the interaction between the CO(5σ) orbital and the surface bands. The surface s-, p-, and d-band contributions to the Pd−CO(5σ) HP are shown in Figure 9. The HP plots in Figure 9 reveal significant s-, p-, and d-band contributions to the Pd−CO(5σ) bonding band at ~ -15 eV.

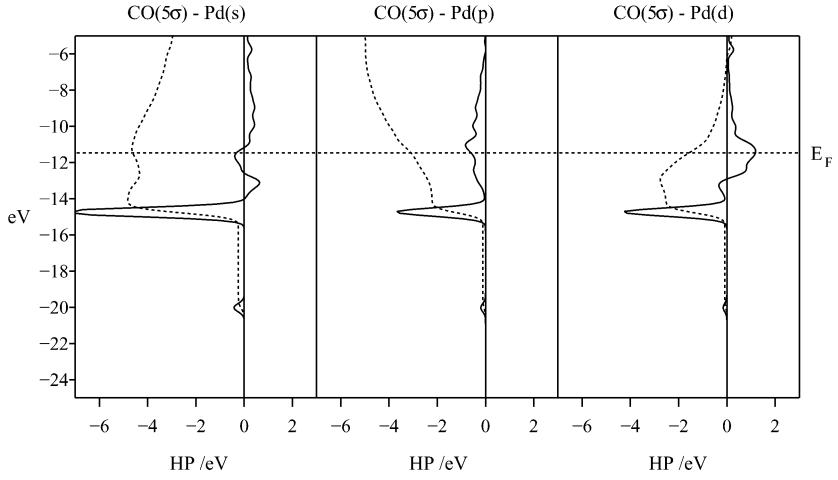

Figure 9. Plots of the surface s-, p-, and d-band contributions to the Pd−CO(5σ) HP.

SCHEME 3

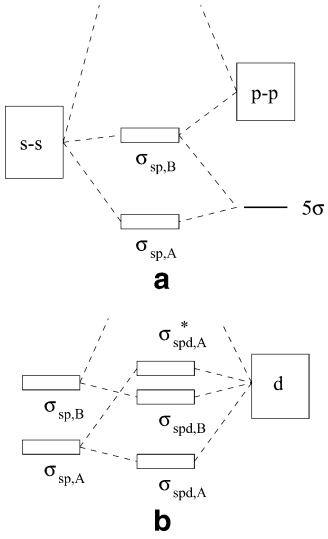

In the case of the d-band component, the corresponding $5\sigma-$d antibonding interactions are distributed about the Fermi level as evidenced by the positive contributions to the d-band component of the Pd−CO(5σ) HP between ~ -13 and ~ -10 eV (Figure 9).

Interpretation of the $5\sigma-$s interaction is somewhat less straightforward. In addition to the $5\sigma-$s bonding states at ~ -15 eV (Figure 9) additional $5\sigma-$s bonding states appear in the vicinity of the Fermi level. The origin of $5\sigma-$s antibonding states both above and below the Fermi level also remains to be clarified. The p-band contribution to the Pd−CO(5σ) interaction is less complex, however the presence of $5\sigma-$p bonding interactions − in addition to those at ~ -15 eV − distributed over a wide energy range both above and below the Fermi level must be accounted for. To account for these observations, it is necessary to propose a model of Pd−CO(5σ) bonding that explicitly details the role of the surface s and p-bands in addition to the long-established role of the d band.[20,22]

The interaction between the low-lying CO(5σ) orbital and the surface s and p bands results from the three-band interaction illustrated in Scheme 3a. In accord with the results of perturbation theory, when two orbitals mix, the higher energy orbital mixes into the lower energy orbital in a bonding way. In contrast, the low energy orbital mixes into the high energy orbital in an antibonding way. Thus, mixing of the s−s bonding band straddling the Fermi level (Figure 6) into the relatively low-lying 5σ band gives rise to $5\sigma-$s bonding states, denoted $\sigma_{sp,A}$ in Scheme 3a. The corresponding $5\sigma-$s antibonding states resulting from mixing of the 5σ band into the higher lying s−s bonding band in an antibonding way are found within the $\sigma_{sp,B}$ band. Subsequent mixing of the p−p bonding band into the relatively low-lying $\sigma_{sp,A}$ and $\sigma_{sp,B}$ bands imparts $5\sigma-$p bonding character into each band. Thus, the bonding contributions made by the s and p bands to the Pd−CO(5σ) bonding band at ~ -15 eV (Figure 9) serve to identify the $\sigma_{sp,A}$ band in the CO/Pd(111) chemisorption system. In addition, the simultaneous existence of $5\sigma-$p bonding and $5\sigma-$s antibonding contributions to the Pd−CO(5σ) HP at ~ -13 eV serves to identify the $\sigma_{sp,B}$ band parentage of states that have subsequently acquired d-band character via mixing of the $\sigma_{sp,B}$ band with the d band. The appearance of $5\sigma-$s bonding states about the Fermi level cannot, however, be rationalized without invoking the surface d-band.

Subsequent introduction of the d band (Scheme 3b) again results in a three-band interaction, in this instance between the surface d band and the $\sigma_{sp,A}$ and $\sigma_{sp,B}$ bands. Again, by the rules of perturbation theory, the low-lying $\sigma_{sp,A}$ band is stabilized on mixing into itself a portion of the higher energy d band in a bonding way as evidenced by the bonding contribution to the $5\sigma-$d HP at ~ -15 eV in Figure 9. The addition of $5\sigma-$d bonding components to the $\sigma_{sp,A}$ band results in its redesignation as the $\sigma_{spd,A}$ band (Scheme 3b). Thus, when we refer to the 5σ band that appears at ~ -15 eV in the DOS for the CO/Pd(111) chemisorption system (Figure 3), we are, in fact, referring to the $\sigma_{spd,A}$ band derived in Scheme 3b. The corresponding $5\sigma-$d antibonding states resulting from mixing of the $\sigma_{sp,A}$ band into the d band are distributed about the Fermi level as shown in Figure 9. The $\sigma_{sp,A}$ band parentage of these states is evidenced by the emergence of bonding contributions to the $5\sigma-$s component of the Pd−CO(5σ) HP and antibonding contributions to the $5\sigma-$d interaction within the same energy window about the Fermi level (Figure 9). Thus, through formation of the $\sigma^*_{spd,A}$ band, it becomes possible to account for the existence of $5\sigma-$s bonding contributions in the vicinity of the Fermi level.

Consider now the interaction between the d band and the $\sigma_{sp,B}$ band. Prior to inclusion of the d band in Scheme 3b, the $\sigma_{sp,B}$ band is comprised of $5\sigma-$p bonding interactions and $5\sigma-$s antibonding interactions. The $5\sigma-$s antibonding character of the $\sigma_{sp,B}$ band emerges in the form of antibonding contributions to the s-band component of the surface−5σ HP below the Fermi level on allowing the $\sigma_{sp,B}$ and d bands to mix. Thus, the $5\sigma-$s antibonding states at ~ -13 eV, in combination with the bonding contributions to the $5\sigma-$p and $5\sigma-$d components of the Pd−CO(5σ) HP at the same energy, serve to locate those states belonging to the $\sigma_{spd,B}$ band, states resulting from the mixing of the $\sigma_{sp,B}$ and d bands in a bonding way (Scheme 3b). The corresponding antibonding states in the form of the $\sigma^*_{spd,B}$ band are found above the Fermi level. Thus it is possible to account for the s-, p-, and d-band contributions to the Pd−CO(5σ) HP shown in Figure 9. The model of Pd−CO(5σ) bonding developed in Scheme 3 demonstrates the way in which the relatively weak interaction between the CO(5σ) orbital and the surface d band can be considered a perturbation of the much more substantial interaction between the 5σ orbital and the surface s and p bands as proposed by Hammer et al.[23]

The CO(4σ) orbital interacts with the surface bands in an analogous manner to the CO(5σ) orbital. However, the effects of the interaction between the CO(4σ) orbital and the surface bands are much less pronounced on account of the relatively poor energy match between the surface bands and the CO(4σ) orbital. The bonding interactions between the CO(4σ) orbital and the surface bands contained within the low-lying 4σ band (Figure 4) and the subsequent tempering of the CO(4σ) contribution to Pd−CO bonding that occurs via mixing with the 5σ band dominate the picture of 4σ interaction with the surface bands.

The construction of an orbital mixing model to describe the interaction between the CO(2π) orbitals and the surface bands is somewhat less involved than the model of Pd−CO(5σ) bonding detailed in Scheme 3. The two-band model presented in Scheme 4a describes the formation of Pd−CO(2π) bonding states via mixing of the CO(2π) orbitals with the surface s and p bands. Prior studies of CO chemisorption on the Cu(111) surface[19] demonstrate that partial filling of the resulting π_{sp} band by electrons from the surface s and p bands is sufficient to account for the π component of Cu−CO bonding.

Subsequent mixing of the π_{sp} band with the d band (Scheme 4b) gives rise to $2\pi-$d bonding states distributed throughout the d band, the π_{spd} band. The corresponding $2\pi-$d antibonding

SCHEME 4

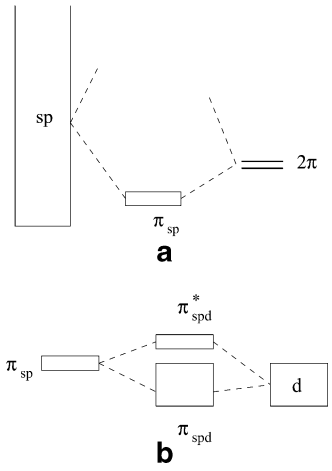

states, the π^*_{spd} band, are found above the Fermi level. On constructing the model of Pd−CO(2π) interaction in this way, it becomes a relatively straightforward matter to account for the bonding and antibonding contributions to the surface s-, p-, and d-band components of the Pd−CO(2π) HP shown in Figure 5. The bonding nature of the interactions between the CO(2π) orbitals and the surface s, p, and d bands contained within the π_{spd} band is manifested in the bonding (negative) contributions to the surface s-, p-, and d-band components of the Pd−CO(2π) HP distributed below ~ -11 eV (Figure 5). The π^*_{spd} band emerges in the form of bonding contributions to both the 2π−s and 2π−p components of the Pd−CO(2π) HP centered around −10 eV (Figure 5). Both of these contributions reflect the π_{sp} band parentage of the π^*_{spd} band. The antibonding contributions to the 2π−d interaction also centered about −10 eV serve to confirm the location of the π^*_{spd} band.

VI. NO Chemisorption

In this section, the focus is on extending the picture of CO chemisorption presented in the previous section to describe and contrast NO chemisorption on the Pd(111) surface. As was the case for CO chemisorption, NO chemisorption at low coverage is modeled by a p(2 × 2)-NO phase with NO chemisorbed on bridging sites. Given the equivalence of the computed Pd−C and Pd−N bond lengths for bridge site chemisorption (Table 1), it becomes possible to directly compare the overlap of individual CO and NO orbitals with the surface bands. Thus, it proves useful to begin an analysis of NO chemisorption by comparing the topology of corresponding CO and NO orbitals. Contour plots of the 5σ and 2π orbitals of CO and NO are shown in Figure 10.

Analysis of the orbitals shown in Figure 10 reveals that the greater electronegativity difference between the atoms in CO results in a more substantial polarization of both the CO 5σ and 2π orbitals toward the carbon atom. Thus, given the equivalence of the Pd−C and Pd−N bond lengths for bridge site chemisorption, we might expect increased overlap and consequently greater interaction, between both the CO 5σ and 2π orbitals and the surface bands. Computing the HPs for the interaction of the 5σ and 2π orbitals of CO and NO with the surface bands reveals that, as anticipated, the NO(5σ) interaction with the surface is smaller than the Pd−CO(5σ) interaction. In contrast, the NO(2π) interaction with the surface is computed to be greater than the CO(2π) interaction. Thus, overlap is not the sole factor determining the magnitude of the interactions between the adsorbate orbitals and the surface bands. Within

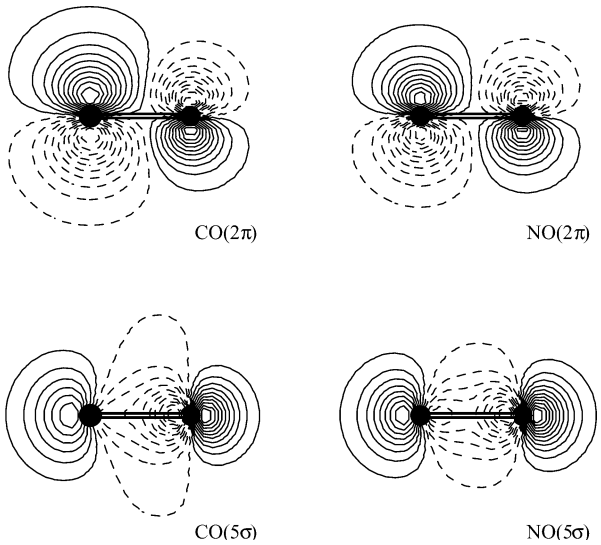

Figure 10. Contour plots of the 5σ and 2π molecular orbitals of CO and NO. The contours are plotted at intervals of 0.01. The outermost contour represents the surface on which the magnitude of the wave function is 0.01.

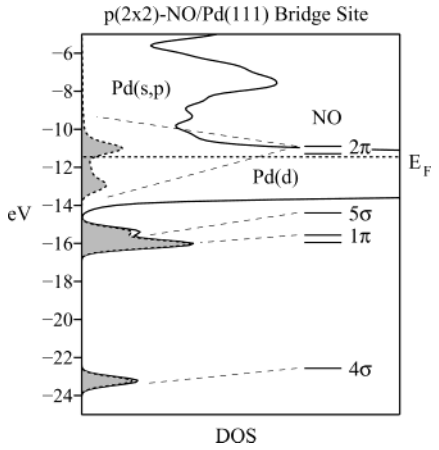

Figure 11. DOS for the p(2 × 2)-NO/Pd(111) chemisorption system with NO chemisorbed in bridging sites. Contributions from the NO orbitals are shown shaded. The molecular orbital energies for an isolated gas-phase NO molecule are superimposed for comparison.

TABLE 6: NO 4σ, 5σ, and 2π Orbital Occupations for p(2 × 2)-NO/Pd(111) Phases with NO Chemisorbed in Top, Bridge, and Hollow Sites

	MO occupation			
NO orbital	top	bridge	HCP hollow	FCC hollow
4σ	1.87	1.85	1.83	1.84
5σ	1.73	1.72	1.72	1.72
2π	1.21	1.65	1.88	1.89

the tightbinding framework employed in this study,[15] the orbital interaction energy is proportional to the square of the orbital overlap and inversely proportional to the energy separation of the interacting orbitals.

Thus, despite a smaller overlap between the NO(2π) orbitals and the surface bands, the improved energy match between the NO(2π) orbitals and the surface d band results in substantially greater 2π−d mixing on chemisorbing NO (Figure 11). Comparison of the distribution of the 2π orbital DOS on chemisorbing CO and NO (Figures 3 and 11 respectively) reveals increased NO(2π) contributions to the 2π−d bonding states distributed throughout the d band. Comparison of the 2π occupations for the NO/Pd(111) chemisorption system (Table

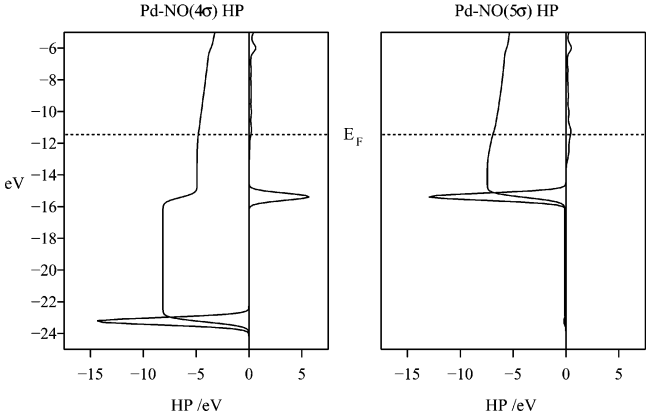

Figure 12. NO(4σ) and NO(5σ) contributions to the Pd−NO bond HP for the p(2 × 2)-NO/Pd(111) chemisorption system with NO chemisorbed in bridging sites.

TABLE 7: Individual NO Orbital Contributions to the Pd−NO Bond HP for the p(2 × 2)-NO/Pd(111) Chemisorption System with NO on Bridging Sites

	Pd−NO HP /eV			
NO orbital	top	bridge	HCP hollow	FCC hollow
3σ	0.124	0.495	0.702	0.707
4σ	−4.484	−4.820	−5.134	−5.102
1π	0.020	−0.524	−0.904	−0.907
5σ	−6.901	−6.952	−7.071	−7.076
2π	−4.732	−9.124	−11.233	−11.183
6σ	−0.098	−0.199	−0.242	−0.241
total	−16.071	−21.124	−23.882	−23.802
4σ + 5σ + 2π	−16.117	−20.896	−23.438	−23.361

6) with those for the CO/Pd(111) chemisorption system (Table 4) demonstrates that increased mixing of the NO(2π) orbitals into the surface d band results in increased back-donation to the NO(2π) orbitals on all sites. Comparison of the CO and NO 2π orbital contributions to surface−adsorbate bonding (Tables 3 and 7 respectively) highlights the increased contribution of the 2π orbitals resulting from increased 2π−d mixing on chemisorbing NO.

The combined effect of a reduction in the NO(5σ) orbital energy and reduced NO(5σ) overlap with the surface bands in rendering the 5σ orbital contribution to Pd−NO bonding less significant than for Pt−CO bonding can also be clearly descerned from Tables 3 and 7. The corresponding reduction in forward donation from the 5σ orbital is reflected in the relatively small reduction in the 5σ orbital occupation for NO on all sites (Table 6).

The increased role of the 4σ orbital in binding NO on all sites is however surprising given the poor energy match between the relatively low-lying NO(4σ) orbital and the surface bands (Figure 11). We have already seen that, on chemisorbing CO, the 4σ and 5σ orbitals interact strongly with the surface bands. Subsequent mixing of the Pd−CO(4σ) bonding band into the higher lying Pd−CO(5σ) bonding band, which, in accord with perturbation theory, occurs in an antibonding way, gives rise to Pd−CO(4σ) antibonding interactions within what was originally the 5σ band.[19] Mixing of the NO 4σ and 5σ orbitals in this way can be clearly seen on plotting the energy resolved contributions to the Pd−NO(4σ) and Pd−NO(5σ) HPs (Figure 12). Despite the substantial reduction in the 4σ contribution to Pd−NO bonding brought about by 4σ−5σ mixing (Figure 12), the 4σ contribution to Pd−NO bonding remains significant as in the case of CO chemisorption. Comparison of the 4σ contribution to the Pd−CO HP (Table 3) and Pd−NO HP (Table 7) reveals an approximately 10% increase in the 4σ contribution for NO binding in all sites. Integration of the 4σ band contributions to Pd−CO and Pd−NO bonding (Figures 4 and 12) reveals that the 4σ orbital interaction with the surface within the low-lying 4σ band is greater on chemisorbing CO. Thus, the ∼10% increase in the net 4σ contribution to surface−adsorbate bonding on binding NO can be attributed to a reduction in 4σ−5σ mixing in the NO/Pd(111) chemisorption system. Computing the energy separation between the 4σ and 5σ orbitals in CO and NO reveals a 2.4 eV larger 4σ−5σ separation in NO. In accord with the results of perturbation theory, the increased energy separation between the interacting orbitals results in a reduction in 4σ−5σ mixing on chemisorbing NO. This is confirmed on integrating the surface−4σ HP for CO and NO through the respective 5σ bands shown in Figures 4 and 12. The 40% reduction in surface-4σ bonding within the 5σ band on chemisorbing NO is indeed less than the corresponding 53% reduction for CO.

TABLE 8: Surface s-, p-, and d-Band Components of the NO 4σ, 5σ, and 2π Orbital Contributions to the Pd−NO Bond HP for the p(2 × 2)-NO/Pd(111) Chemisorption System with NO in Bridging Sites

	surface band		
NO orbital	Pd(s)	Pd(p)	Pd(d)
4σ	−2.273	−2.190	−0.356
5σ	−3.000	−2.828	−1.123
2π	−1.820	−1.846	−5.458

TABLE 9: Decomposition of the Computed NO Chemisorption Energies for p(2 × 2)-NO/Pd(111) Chemisorption Systems with NO Chemisorbed in Top, Bridge, and Hollow Sites[a]

			ΔHP(Pd-Pd)		
site	HP(Pd-NO)	ΔHP(N-O)	ΔHP_s	ΔHP_{s-u}	E_{chem}
top	−16.07	0.24	−0.01	−0.26	−16.10
bridge	−21.12	2.51	1.41	0.19	−17.01
hcp	−23.88	3.92	1.87	0.45	−17.64
fcc	−23.80	3.98	2.14	0.35	−17.33

[a] All HPs are in units of eV. The change in Pd−Pd bonding within the slab, ΔHP(Pd−Pd), is decomposed to reveal the change in Pd−Pd bonding within the surface (ΔHP_s) and between the surface and underlayer (ΔHP_{s-u}).

Table 8 details the surface s-, p-, and d-band contributions to the interaction between the NO 4σ, 5σ, and 2π orbitals and the surface. Analysis of Table 8 reveals that, as was the case for CO, both the NO 4σ and 5σ orbitals interact principally with the surface s and p bands. Again by analogy with CO, Table 8 reveals that the substantial bonding interaction between the NO(2π) orbitals and the surface appears to be principally the result of interactions with the surface d band. Analysis of the surface s-, p-, and d-band contributions to the HP between the NO(2π) orbitals and the surface (not shown) reveals the potential for substantial 2π bonding interactions involving both the surface s and p bands in the form of 2π−s and 2π−p bonding states analogous to those for CO that are found above the Fermi level (Figure 5). Thus, the picture developed previously to describe the role of the 4σ, 5σ, and 2π orbitals in Pd−CO bonding can be readily applied to describe NO chemisorption on the Pd(111) surface.

The energetic consequence of increased back-donation and reduced forward donation on chemisorbing NO is best quantified by computing the chemisorption energy for NO chemisorption using eq 5. The chemisorption energies computed for NO chemisorbed in top, bridge, and hollow sites are summarized in Table 9. Examination of Table 9 reveals a preference for hollow site chemisorption over bridge site chemisorption

TABLE 10: Chemisorption Induced Changes in Pd−Pd Bond HPs within the Surface on Forming p(2 × 2)-CO and p(2 × 2)-NO Phases with CO and NO Occupying Bridging Sites

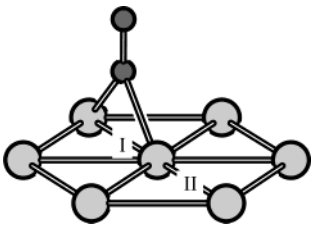

	ΔHP(bondI)/eV		ΔHP(bondII)/eV	
Pd−Pd bond component	CO/Pd	NO/Pd	CO/Pd	NO/Pd
s−s	0.24	0.32	0.16	0.13
s−p	0.04	0.09	0.01	−0.02
s−d	0.27	0.30	0.02	−0.01
p−p	−0.05	−0.04	−0.03	−0.03
p−d	0.21	0.26	−0.03	−0.03
d−d	0.05	0.00	−0.12	−0.18
total	0.76	0.94	0.01	−0.15

consistent with the results of previous computational studies.[9,17] Comparison of the CO and NO chemisorption energies computed by the HP method (Tables 2 and 9, respectively) reveals that the computed chemisorption energies for NO chemisorbed in hollow and bridging sites are consistently greater than for CO in agreement with the results of prior DFT studies.[17,25] In addition, the relatively large reduction in the NO chemisorption energy on moving NO from bridging to top sites computed using the HP method mirrors that computed by Honkala et al. using DFT methods.[17] Comparison of the chemisorption energies for CO and NO chemisorbed in hcp and fcc sites (Tables 2 and 9 respectively) reveals an increased preference for NO chemisorption in hcp sites over fcc sites. This finding is reflected in the increased stability of the CO(fcc)/NO(hcp) phase of the c(4 × 2)-CO,NO/Pd(111) chemisorption system over the CO(hcp)/NO(fcc) phase as computed by Honkala et al. using DFT methods.[17] However, the more substantial preference for NO chemisorption in hcp sites over fcc sites (Table 9) does contrast the modest 0.02 eV preference for NO chemisorption in fcc sites over hcp sites at one-quarter coverage computed by Honkala et al.[17] and the equally modest 0.01 eV preference for NO chemisorption in hcp sites over fcc sites at one-third coverage computed by Hansen et al.[9]

A site-by-site comparison of the computed chemisorption energies for CO (Table 2) and NO (Table 9) reveals increased Pd−CO and Pd−NO bonding with increasing adsorbate coordination. On all sites, Pd−NO bonding is computed to be stronger than Pd−CO bonding. Analysis of the individual CO and NO orbital contributions to Pd−CO and Pd−NO bonding (Tables 3 and 7 respectively) reveals that the increased strength of Pd−NO bonding is primarily the result of increased mixing between the NO(2π) orbitals and the surface bands on all sites. As demonstrated previously, increased mixing between the NO(2π) orbitals and the surface d band results in increased back-donation (Tables 4 and 6) and correspondingly greater reductions in bonding within chemisorbed NO on all sites.

A site-by-site comparison of the Pd−Pd bonding changes accompanying CO and NO chemisorption (Tables 2 and 9 respectively) reveals that the degree of Pd−Pd bond weakening on chemisorbing NO is, on the other hand, consistently less than that accompanying CO chemisorption. On balance, the increased reduction in N−O bonding resulting from increased back-donation is not, however, sufficient to offset the combined

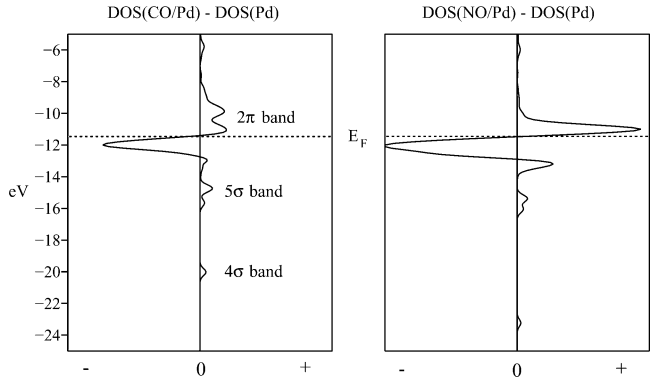

Figure 13. DOS difference (DOS(X/Pd) − DOS(Pd); X = CO,NO) for the d-orbitals of the Pd atoms in the surface layer on forming p(2 × 2)-CO (left panel) and p(2 × 2)-NO (right panel) phases with adsorbates on bridging sites.

effects of increased surface−adsorbate bonding and reduced Pd−Pd bond weakening accompanying NO chemisorption. In this way the NO chemisorption energy, as computed by HP methods, is consistently greater than that for CO on all sites.

VII. Chemisorption Induced Changes in Pd−Pd Bonding

To account for the systematic decrease in Pd−Pd bond weakening that occurs on chemisorbing NO in top, bridge, and hollow sites, it proves instructive to compute and contrast the changes in each of the s−s, s−p, p−p, s−d, p−d, and d−d components of the surface bonds in the vicinity of chemisorbed CO and NO. Table 10 details the changes in Pd−Pd bonding within the bond directly below bridging CO and NO (bond I) and within an adjacent Pd−Pd bond (bond II) on chemisorbing CO and NO in bridging sites. Analysis of the Pd−Pd bond HP changes summarized in Table 10 reveals that Pd−Pd bonding directly below bridging CO or NO is substantially weakened by the chemisorption process. On chemisorbing CO or NO, the s−s, s−d, and p−d components of bond I are most affected. In contrast, analysis of the bond HP changes within bond II reveals a relatively modest perturbation of Pd−Pd bonding that is largely confined to the s−s and d−d components of the bond.

On chemisorbing CO, the increase in the d−d component of bond II effectively offsets the reduction in s−s bonding with the result that the bond weakens by a modest 0.01 eV. In the case of NO chemisorption, the reduction in s−s bonding within bond II on chemisorbing NO is not sufficient to offset a more substantial increase in d−d bonding that results in a net 0.15 eV *increase* in the bond HP for bond II. The perturbation in Pd−Pd bonding within other Pd−Pd bonds about chemisorbed NO, both within the surface layer and between the surface layer and underlayer, mirrors that within bond II (Table 10). Summing the Pd−Pd bond HP changes about chemisorbed CO and NO reveals that the reduction in Pd−Pd bond weakening adjacent to chemisorbed NO more than compensates for the greater reduction in Pd−Pd bonding directly below NO (Table 10). Thus, the reduction in Pd−Pd bond weakening that accompanies NO chemisorption in top, bridge, and hollow sites is the result of increases in the d−d component of Pd−Pd bonding in those bonds adjacent to the adsorbate site. In this context, the term adjacent refers only to those Pd−Pd bonds that share a surface atom with the adsorbate. The extent of Pd−Pd bond weakening in bonds adjacent to chemisorbed CO or NO is thus, primarily, a function of the extent to which the adsorbate orbitals mix with the surface d band.

On chemisorbing CO or NO, the adsorbate 2π orbitals interact with the surface s, p, and d bands according to the mixing model

presented in Scheme 4, parts a and b. The resulting π_{spd} and π^*_{spd} bands can be detected via their influence on the surface d band. Figure 13 demonstrates the reduction in the d-band DOS just below the Fermi level that accompanies formation of the π_{spd} and π^*_{spd} bands. Formation of the π_{spd} band is evidenced by the buildup of d-band DOS within the surface layer between -13 and -14 eV. Analogously formation of the π^*_{spd} band is evidenced by the buildup of d-band DOS above the Fermi level in the energy range from ~ -10 to -11 eV. The increased buildup of d-band DOS within both the π_{spd} and π^*_{spd} bands on chemisorbing NO (Figure 13) is further evidence of increased $2\pi-$d mixing.

The relatively large increase in the d−d component of Pd−Pd bonding for bond II on chemisorbing NO can be attributed to increased $2\pi-$d mixing on chemisorbing NO. However, to be able to translate increased $2\pi-$d mixing into an increase in the d−d bonding component of those Pd−Pd bonds about chemisorbed NO, it is necessary to examine the nature of the surface d-states contributing to $2\pi-$d mixing. Analysis of the surface d-band DOS difference in Figure 13 reveals that $2\pi-$d mixing involves states from the upper portion of the surface d-band. As demonstrated by the d−d component of the Pd−Pd HP in Figure 8, the upper portion of the surface d-band contains states responsible for d−d antibonding interactions between Pd atoms in the surface. Thus, on chemisorbing CO or NO, the interaction between the adsorbate 2π orbitals and the surface d band serves to depopulate those d−d antibonding states contributing to the π^*_{spd} band. In this way, increased $2\pi-$d mixing on chemisorbing NO results in a reduction in d−d antibonding contributions to Pd−Pd bonds about chemisorbed NO.

Reducing the availability of the d-orbitals contributing to d−d antibonding interactions on the Pd atoms bonded to the adsorbate serves to reduce the potential for d−d antibonding interactions within those Pd−Pd bonds involving Pd atoms bonded to the adsorbate. The reduction is particularly severe in the case of those Pd−Pd bonds for which both Pd atoms are directly bonded to the adsorbate. Thus we might expect to observe a substantial increase in the d−d component of Pd−Pd bond I on chemisorbing either CO or NO. Analysis of the change in the d−d component of bond I in Table 10 reveals, instead, that the anticipated increase in the d−d component of bond I is masked by the reduction in d−d bonding that results from depopulation of those d−d bonding states interacting with the adsorbate σ orbitals in accord with the mixing model proposed in Scheme 3, parts a and b.

The mixing model proposed in Scheme 3, parts a and b also accounts for the reduction in the s−s bonding components of bonds I and II. On chemisorbing CO or NO in bridging sites, the adsorbate σ orbitals have the correct symmetry to interact with only those surface states that contribute to s−s bonding interactions within bond I. Thus, the σ interaction between the adsorbate and the surface serves to depopulate those states contributing to s−s bonding interactions within bond I. Reducing the availability of the s orbitals involved in s−s bonding on those Pd atoms bonded to the adsorbate serves to reduce s−s bonding within those Pd−Pd bonds involving Pd atoms bonded to the adsorbate. In this way, the increased reduction in the s−s component of Pd−Pd bond II on chemisorbing CO is seen to be the result of increased mixing between the CO(5σ) orbital and the surface s-band. The effect of reducing the availability of the s orbitals on those Pd atoms bonded to the adsorbate is once again found to be more substantial within those Pd−Pd bonds for which both Pd atoms are bonded to the adsorbate. Analysis of the reduction in the s−s contribution to bonding within bond I on chemisorbing CO and NO (Table 10) reveals this to be the case. However, the increased reduction in s−s bonding contributions within bond I resulting from increased $5\sigma-$s mixing on chemisorbing CO is masked by an additional reduction in the s−s contribution to bond I on chemisorbing NO. To account for the additional reduction in s−s bonding within bond I for NO, it becomes necessary to consider the nature of the surface s states that mix with the adsorbate 2π orbitals. On chemisorbing CO or NO in bridging sites, only those states that contribute to s−s antibonding between the Pd atoms in bond I have the correct symmetry to contribute to the $2\pi-$s bonding interactions within the π_{spd} band. In this way, increased 2π mixing with the surface bands on chemisorbing NO results in increased occupation of states that contribute s−s antibonding interactions to bond I. Thus, the relatively large reduction in s−s bonding contributions to bond I on chemisorbing NO is the combined result of depopulating s−s bonding states via interaction with the adsorbate σ orbitals and increased population of s−s antibonding states via increased mixing with the NO(2π) orbitals.

Thusfar, only the variations in the s−s and d−d components of Pd−Pd bonding accompanying chemisorption have been discussed. Analysis of Table 10 also reveals substantial reductions in the s−d and p−d components of Pd−Pd bonding within bond I on chemisorbing CO or NO. In light of the discussions of sd mixing and pd mixing accompanying Scheme 2, it follows that a reduction in either the s−s or d−d bonding contributions to Pd−Pd bonding distributed throughout the lower portion of the d band (Figure 8) will serve to reduce the s−d bonding contributions to Pd−Pd bonding. In this way, the reduction in s−d bonding within bond I is the combined result of reductions in both the s−s and d−d bonding contributions due to mixing with the adsorbate σ orbitals. Further, analysis of the p−d contributions to the Pd−Pd bond HP shown in Figure 8 reveals that a reduction in either the d−d bonding or antibonding contributions to Pd−Pd bonding could result in a reduction in the p−d bonding contributions distributed throughout the d band (Figure 8). In this way, the decrease in p−d contributions to bonding within bond I is seen to result from a reduction in both the d−d bonding and antibonding components via their respective mixing with the adsorbate σ and π orbitals.

Thus, having developed detailed models of Pd−Pd bonding within the slab and the interaction between the adsorbate orbitals and the surface bands, it has proved possible to rationalize the changes in Pd−Pd bonding about the adsorbate that accompany chemisorption.

VIII. Conclusion

A bond-by-bond partitioning of the electronic structure changes accompanying CO and NO chemisorption on the Pd(111) surface has been used to verify the preference for CO and NO chemisorption in hollow sites. By choosing to employ the HP method, it has been possible to quantify the role of surface−adsorbate bonding and the accompanying changes in bonding that occur within both the adsorbate and the surface, in producing a preference for chemisorption in hollow sites. The preference for CO and NO chemisorption in hollow sites is seen to result from the inability of the reduction in bonding, within both the adsorbate and the surface, to counter the increase in Pd−CO and Pd−NO bonding with increasing adsorbate coordination.

Increased mixing of the NO(2π) orbitals with the surface d band is determined to be the primary factor responsible for

TABLE 11: Extended Hückel Parameters Used in This Study[a]

atom	orbital	H_{ii}/eV	ζ_1	ζ_2	c_1	c_2
Pd	4d	−12.3	5.983	2.613	0.5264	0.6373
	5s	−9.2	2.190			
	5p	−5.5	2.190			
C	2s	−21.4	1.625			
	2p	−11.4	1.625			
N	2s	−26.0	1.950			
	2p	−13.4	1.950			
O	2s	−32.3	2.275			
	2p	−14.8	2.275			

[a] The coefficients c_1 and c_2 define the contributions of the individual slater type orbitals in the double zeta expansion used to represent the Pd 4d orbitals.

increased surface−adsorbate bonding with NO on all sites. The increase in 2π−d mixing on chemisorbing NO, in turn, serves to increase back-donation to the NO(2π) orbitals on all sites. However, the increased reduction in N−O bonding that results from increased back-donation is not sufficient to offset the combined effects of relatively strong Pd−NO bonding and reduced Pd−Pd bond weakening about chemisorbed NO, with the result that the computed NO chemisorption energy exceeds that for CO on all sites in accord with the results of prior DFT studies.

Within the molecular orbital description of chemisorption presented in this work, increased mixing of the NO(2π) orbitals with the surface d band is also found to be the principal factor behind the relatively minor perturbation of Pd−Pd bonding that accompanies NO chemisorption on all sites. Mixing of the adsorbate 2π states with the d band involves those states that contribute to d−d antibonding interactions within Pd−Pd bonds about the adsorbate. Thus, increased 2π−d mixing on chemisorbing NO serves to reduce d−d antibonding contributions to the Pd−Pd bonds about chemisorbed NO and, in so doing, reduce the extent of Pd−Pd bond weakening. In this way, the extent to which π acceptors such as CO and NO weaken bonding within the surface is determined by the extent to which the π-acceptor function mixes with the surface d band. More generally, the model of CO and NO chemisorption presented in this study can be used to both rationalize and quantify the extent to which the σ-donor and π-acceptor functions of adsorbates perturb the electronic structure of the surface about the adsorbate. In the case of a σ-donor function, mixing with the surface s band serves to reduce s−s bonding contributions in surface bonds about the adsorbate. However, in the presence of a π-acceptor function, significant mixing between the π function and the surface d band may serve to significantly reduce the extent of bond weakening within the surface.

Thus, the present contribution not only provides detailed insight into the nature of the preference for chemisorption in hollow sites, the model of surface−adsorbate bonding developed affords an understanding of the mechanism by which adsorbates modify the surface and thus, potentially, the chemisorption of a neighboring adsorbate.

Acknowledgment. The author acknowledges The College of Wooster for its support of this work.

Appendix

The extended Hückel parameters used in this study are summarized in Table 11.

References and Notes

(1) Giessel, T.; Schaff, O.; Hirschmugl, C. J.; Fernandez, V.; Schindler, K.-M.; Theobald, A.; Bao, S.; Lindsay, R.; Berndt, W.; Bradshaw, A. M.; Baddeley, C.; Lee, A. F.; Lambert, R. M.; Woodruff, D. P. *Surf. Sci.* **1998**, *406*, 90.
(2) Ohtani, H.; Van Hove, M. A.; Somorjai, G. A. *Surf. Sci.* **1987**, *187*, 372.
(3) Loffreda, D.; Simon, D.; Sautet, P. *Surf. Sci.* **1999**, *425*, 68.
(4) Sautet, P.; Rose, M. K.; Dunphy, J. C.; Behler, S.; Salmeron, M. *Surf. Sci.* **2000**, *453*, 25.
(5) Bradshaw, A. M.; Hoffmann, F. M. *Surf. Sci.* **1978**, *72*, 513.
(6) Tueshaus, M.; Berndt, W.; Conrad, H.; Bradshaw, A. M.; Persson, B. *Appl. Phys. A* **1990**, *51*, 91.
(7) Kuhn, W. K.; Szanyi, J.; Goodman, D. W. *Surf. Sci.* **1992**, *274*, L611.
(8) Szanyi, J.; Kuhn, W. K.; Goodman, D. W. *J. Vac. Sci. Technol. A* **1993**, *11*, 1969.
(9) Hansen, K. H.; Sljivancanin, Z.; Hammer, B.; Laegsgaard, E.; Besenbacher, F.; Stensgaard, I. *Surf. Sci.* **2002**, *496*, 1.
(10) Loffreda, D.; Simon, D.; Sautet, P. *J. Chem. Phys.* **1998**, *108*, 6447.
(11) Conrad, H.; Ertl, G.; Kuppers, J.; Latta, E. E. *Surf. Sci.* **1977**, *65*, 235.
(12) Bertolo, M.; Jacobi, K. *Surf. Sci.* **1990**, *226*, 207.
(13) Chen, P. J.; Goodman, D. W. *Surf. Sci.* **1993**, *297*, L93.
(14) Wickham, D. T.; Banse, B. A.; Koel, B. E. *Surf. Sci.* **1991**, *243*, 83.
(15) Glassey, W. V.; Papoian, G. A.; Hoffmann, R. *J. Chem. Phys.* **1999**, *111*, 893.
(16) Glassey, W. V.; Hoffmann, R. *J. Chem. Phys.* **2000**, *113*, 1698.
(17) Honkala, K.; Pirila, P.; Laasonen, K. *Surf. Sci.* **2001**, *498*, 72.
(18) Monkhorst, H. J.; Pack, J. D. *Phys. Rev. B* **1976**, *13*, 5188.
(19) Glassey, W. V.; Hoffmann, R. *J. Phys. Chem. B* **2001**, *105*, 3245.
(20) Blyholder, G. *J. Phys. Chem.* **1964**, *68*, 2772.
(21) Wong, Y.-T.; Hoffmann, R. *J. Phys. Chem.* **1991**, *95*, 859.
(22) Sung, S.-S.; Hoffmann, R. *J. Am. Chem. Soc.* **1985**, *107*, 578.
(23) Hammer, B.; Morikawa, Y.; Norskov, J. K. *Phys. Rev. Lett.* **1996**, *76*, 2141.
(24) Bagus, P. S.; Pacchioni, G. *Surf. Sci.* **1992**, *278*, 427.
(25) Hammer, B *J. Catal.* **2001**, *199*, 171.